Table S1. Structural statistics for the final 20 NMR structure of MIP-3α in water

No. of distance restraints (Overall)	Chemokine	Peptide SDS
Unambiguous NOEs	1827	365
Ambiguous NOEs	455	100
No. of broad dihedral restraints	64	14
RMS distances from ideal values		
Bonds (Å)	$5.6 \times 10^{-3} \pm 1.5 \times 10^{-4}$	$3.4 \times 10^{-3} \pm 5.3 \times 10^{-5}$
Angles (°)	$6.0 \times 10^{-1} \pm 2.3 \times 10^{-2}$	$5.8 \times 10^{-1} \pm 2.7 \times 10^{-3}$
Impropers (°)	$1.9 \pm 1.3 \times 10^{-1}$	$2.5 \times 10^{-1} \pm 5.7 \times 10^{-3}$
Van der Waals (kcal/mol)	112.9 ± 10.1	$7.4 \pm 5.1 \times 10^{-1}$
Distance restraints		
Unambiguous (Å)	$3.0 \times 10^{-2} \pm 2.6 \times 10^{-3}$	$2.2 \times 10^{-2} \pm 4.6 \times 10^{-4}$
Ambiguous (Å)	$2.6 \times 10^{-2} \pm 2.4 \times 10^{-3}$	$4.7 \times 10^{-3} \pm 4.0 \times 10^{-3}$
All distance restraints (Å)	$2.9 \times 10^{-2} \pm 2.1 \times 10^{-3}$	$2.0 \times 10^{-2} \pm 4.0 \times 10^{-4}$
Dihedral restraints (°)	$5.4 \times 10^{-1} \pm 2.1 \times 10^{-1}$	$3.5 \times 10^{-2} \pm 4.7 \times 10^{-2}$
Non-bonded energies		
Electronic (kcal/mol)	-2086.2 ± 59.8	-560.3 ± 23.3
Van der Waals (kcal/mol)	-624.1 ± 16.0	-166.3 ± 2.8
Ramachandran (%)[a]		
Most favored	77.2	78.1
Additionally allowed	22.3	21.9
Generously allowed	0.5	0.0
Disallowed	0.0	0.0
Global r.m.s. distance (Å)		
Backbone[b]	0.492	0.554
Heavy Atom[b]	1.00	1.110
vs. human X-ray structure (1M8A)[c]	1.77	N/A
vs. human X-ray structure (2HCI)[c]	1.64	N/A
vs. murine NMR structure (1HA6)[c]	2.31	N/A

[a] As determined by Procheck

[b] Calculated by MOLMOL for residues 6-65 and 4-16 for the protein and peptide, respectively

[c] Against lowest energy solution structure, backbone atoms of residues 6-65

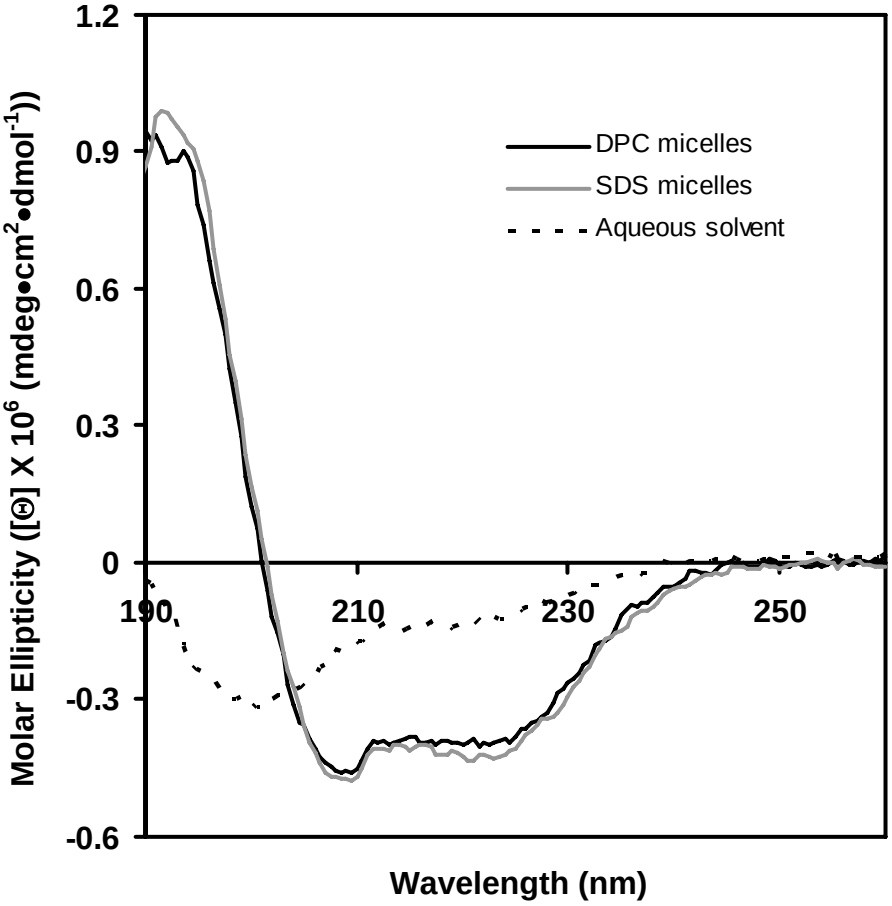

Figure S1. CD spectra of the C-terminal MIP-3α peptide in water, SDS micelles, and in DPC micelles. In aqueous solution, the peptide displays an unstructured curve, while in SDS and DPC it shows characteristically α-helical signals, with minima at about 222 nm and 208 nm. Peptide concentration was 10 μM, pH 7.0.

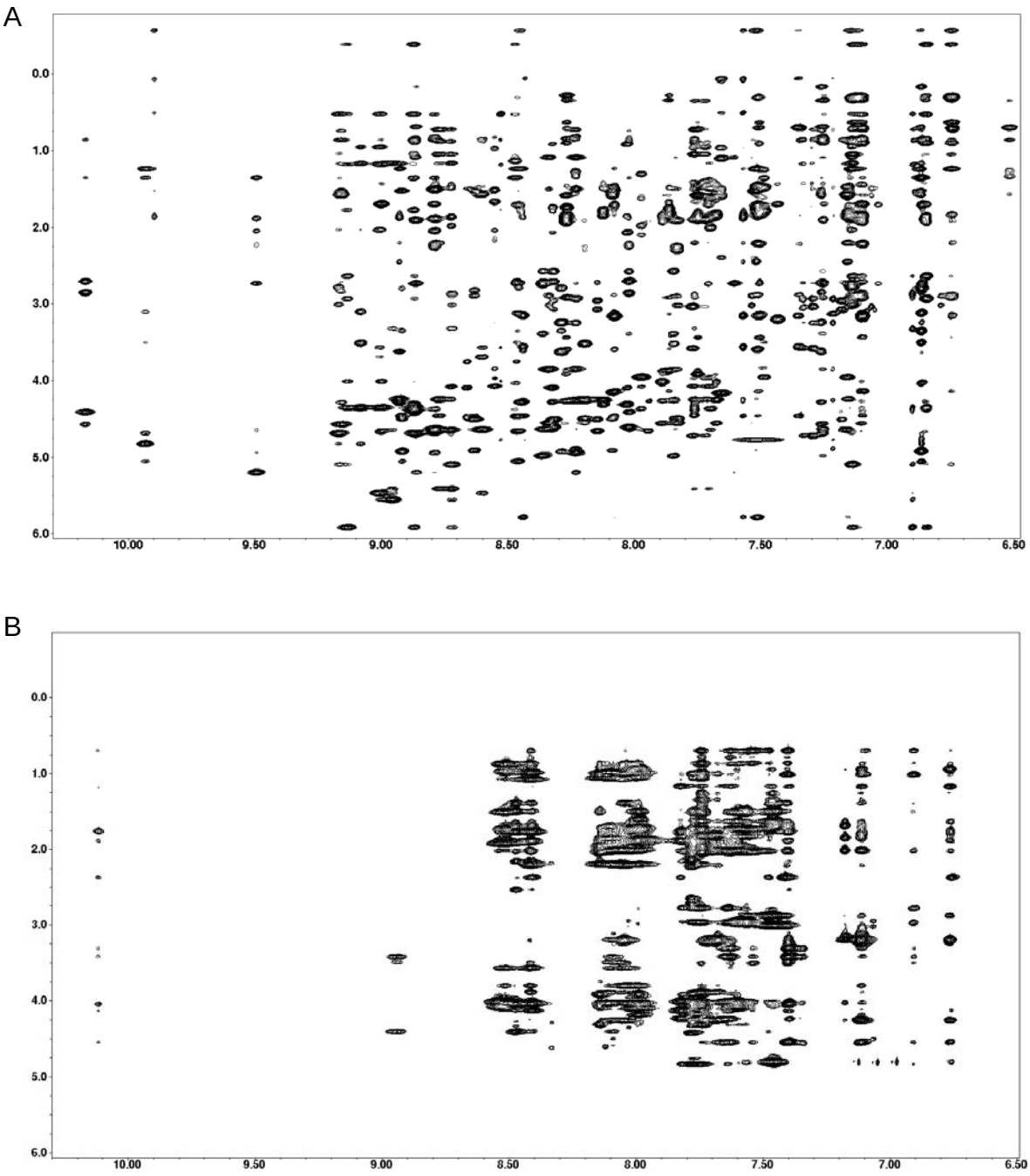

Figure S2. NOESY spectra of intact MIP-3α protein (A) and its 20 residue C-terminal peptide (B). Excellent signal dispersion is seen in the intact protein, while there is some overlap for the peptide due to the broader linewidths caused by the SDS micelles. Nevertheless, predominantly unambiguous assignment of peaks was possible.

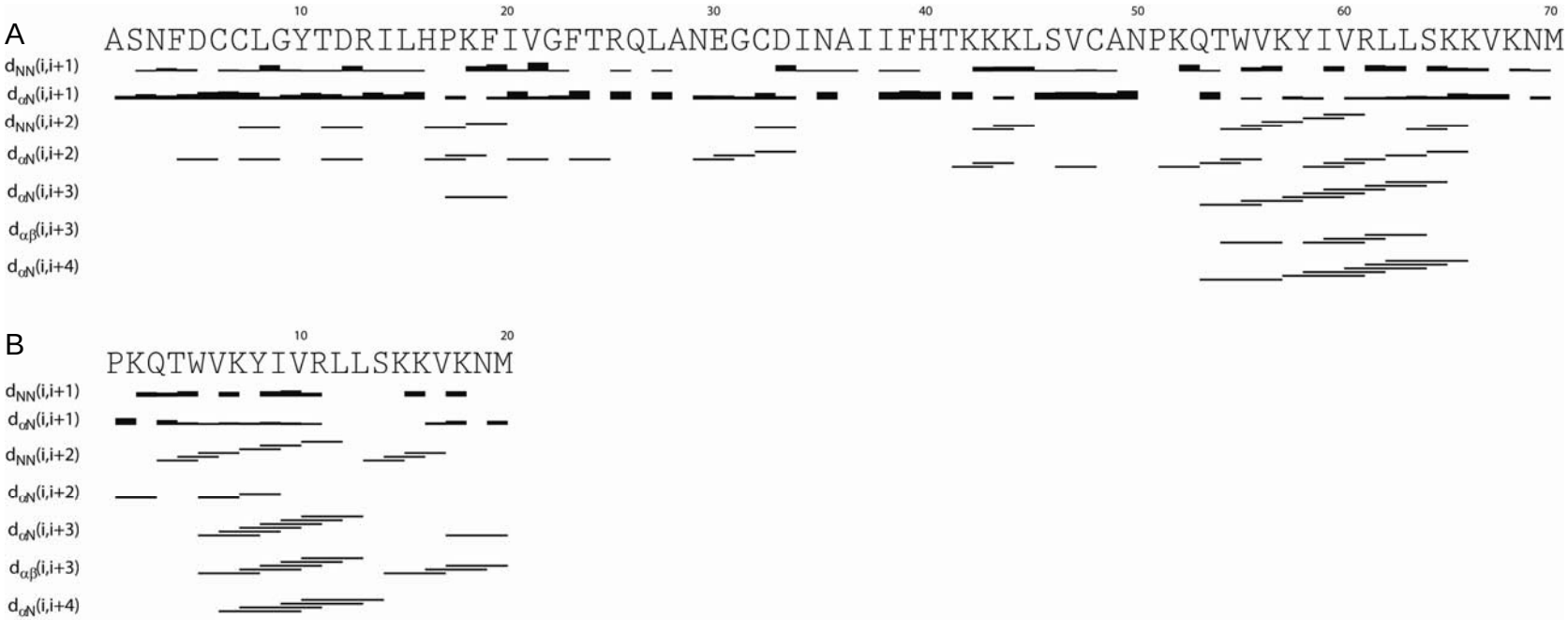

Figure S3. NOE interaction profile for the unambiguous interactions used in the final structure calculations. α-helical regions show the typical medium range interactions of *i*, *i*+3 and *i*, *i*+4.

A

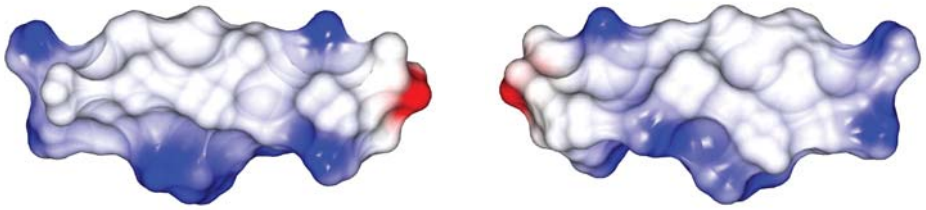

B

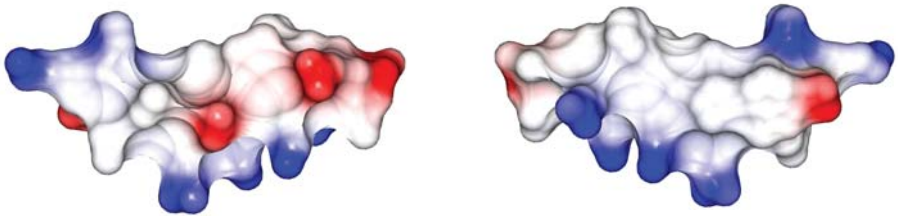

Figure S4. Electrostatic surface plots of the C-terminal peptides of MIP-3α (A) and IL-8 (B). The left hand plots are shown with the N-termini on the left, while the right hand plots are the same peptides rotated by 180 along the y-axis. Positively charged surfaces are shown in blue, negative surfaces in red and hydrophobic areas in white. The plots highlight the amphipathic character of the MIP-3α peptide as well as an increased amount of negative charges in the IL-8 peptide. For IL-8, the 20 most C-terminal residues of PDB ID 1IL8 were used. Plots prepared using CCP4mg (60).

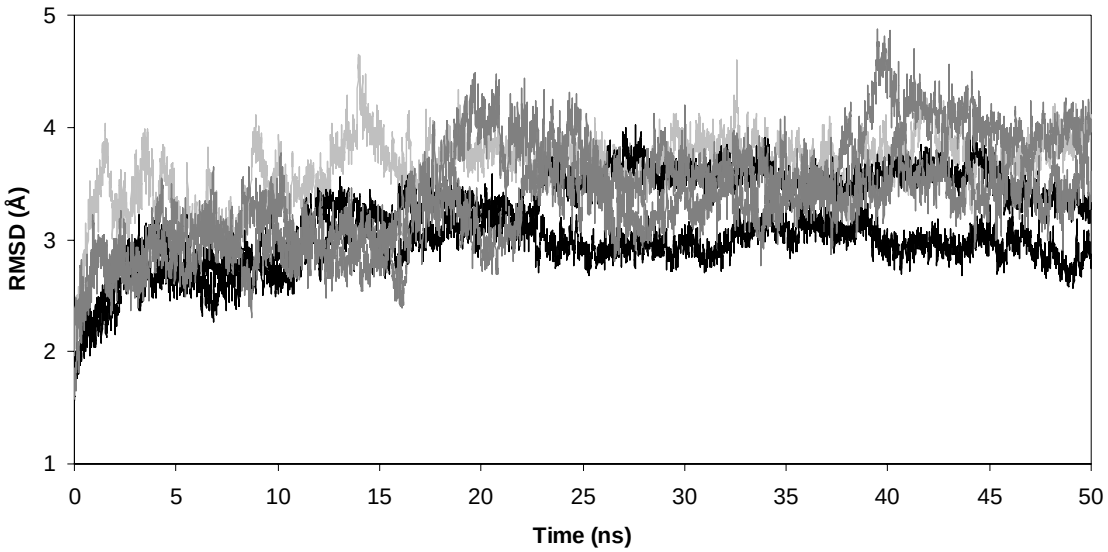

Figure S5. RMSD plots of the MD simulations of MIP-3α, residues 1-65. Typical for this type of simulation, the RMSD values increase initially but stabilize shortly thereafter. Due to the equilibration phase, certain analyses were only conducted on the last 30ns of the simulations. The plots for the dimer simulation are shown in black, for monA and monB are shown in dark grey, while the plot for the NMR structure simulation is depicted in light grey.

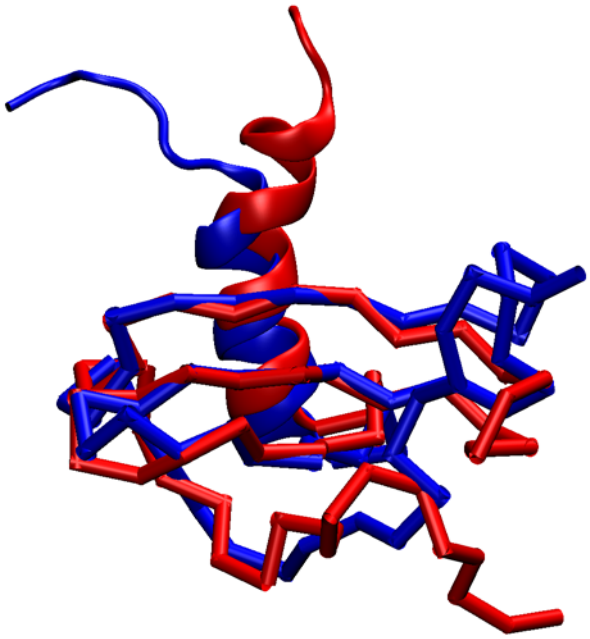

Figure S6. Comparison of the two NMR solution structures of human (blue) and murine (red; PDB ID 1HA6) MIP-3α overlaid on the backbone atoms of the β-strands. The largest differences are seen in the flexible N-terminus and 30s loop. The C-terminal α-helix in the murine structure is oriented more orthogonal to the β-strands compared to the human NMR and crystal structures of MIP-3α.

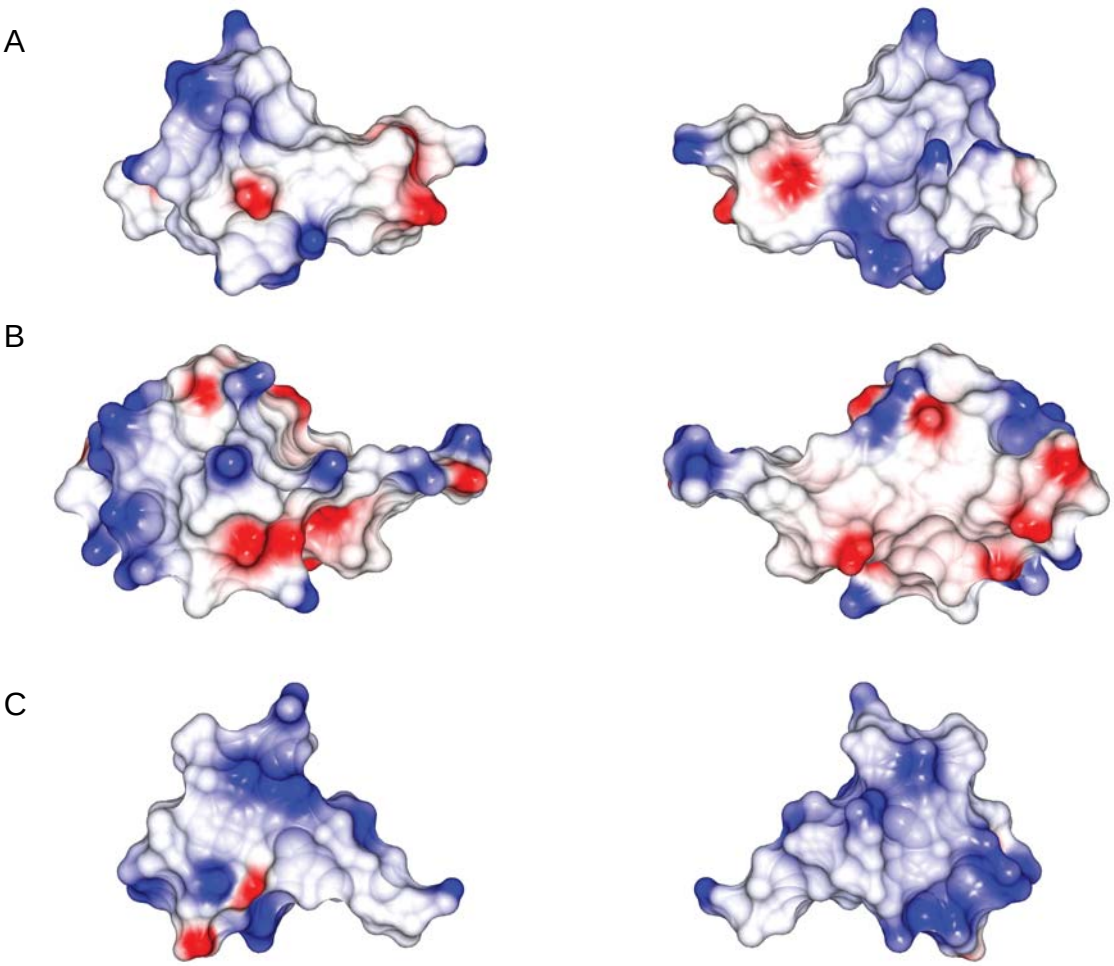

Figure S7. Electrostatic surface profiles of monomeric MIP-3α (A), IL-8 (B), and HBD3 (C) displaying positive charges in blue and negative charges in red. The MIP-3α plot on the left is presented in the same orientation as the ribbon diagram in Fig. 2A, while all three plots on the right hand side represent the proteins flipped 180° along the y-axis. Notice the amphipathic profile of MIP-3α and the increased positive charges on HBD3 compared to IL-8. Surface plots were created with CCP4mg (60).